VARIATIONS IN STRUCTURE OF SUBTROPICAL CURRENT SYSTEM ACCOMPANYING A DEEP POLAR OUTBREAK

CHESTER W. NEWTON

National Center for Atmospheric Research,[1] Boulder, Colo.

ABSTRACT

On February 4, 1960, a polar air mass penetrated in depth southward to the latitude of a trough in the subtropical jet stream. The subtropical and polar fronts amalgamated into a remarkably deep inversion, with temperatures as high as −16° C. at 340 mb., much warmer than the tropical air farther south.

A brief discussion is given of the influence of flow curvature, and of curvature variation with height, on the vertical shear of the wind. The actual shear differed in certain localities, by a factor of two to five, from the geostrophic thermal shear.

Temporary retrogression of the subtropical trough was accompanied by pronounced variations of kinematic and thermal structure, which were in some ways similar to those observed when a minor trough deepens into a major trough of the polar-front wave system. This retrogression was preceded by a westward movement of the wind-speed maximum upstream, and followed by a westward movement of the one downstream. The subtropical front was strong on the western side of the trough and absent on the eastern side early in the development; the reverse was true in later stages.

1. INTRODUCTION

When minor troughs deepen upstream from and replace existing major troughs in the middle-latitude westerlies, asymmetrical structures are generally observed which change in a regular sequence [10]. During the earlier stages, winds near the tropopause level are strongest on the upstream side of the deepening trough. After the trough has achieved full development, the jet stream reaches greatest intensity on the eastern side. A regular sequence, of more or less the same kind, is observed in the locations where the polar front is well developed in the upper troposphere [6].

One of the aims of the present investigation was to discover to what extent regular changes of this sort characterize the subtropical jet stream. In order to capture as much of a full wavelength as possible within the observational network, so as to examine events both upstream and downstream, situations were selected wherein troughs in the subtropical wave system were located near 100° W., central to the North American network. Moreover, since the waves of the subtropical jet stream normally remain almost fixed except when they are interacted with by waves of the middle-latitude westerlies [3], a requirement was that a polar-front trough deepen far enough south to have such an influence. Although such an interaction is most common between polar-front troughs and subtropical jet-stream crests, for the sake of symmetry within the aerological network it was considered desirable that the polar-front troughs coincide with the subtropical troughs. Only the case for February 4, 1960, the most extreme of these cases from the standpoint of intensity of frontal development, is described below. The other two (December 14–16, 1960, and January 11–14, 1961) were qualitatively similar in regard to the principal aspects described below.

2. EXTREME FRONTAL DEVELOPMENT WHERE POLAR FRONT AND SUBTROPICAL FRONT OSCULATE

The synoptic situation at 0000 GMT February 4, 1960, is shown in figure 1. At 500 mb., a cut-off cold Low lay nearly above the surface cyclone. At 250 mb., the warmest air was located a little south of the cold air center in the middle troposphere; at 150 mb. no closed circulation center was present.

At this time, the polar-air trough had come into juxtaposition with the trough in the subtropical jet stream. A partial history of the development is summarized in figure 2 (see also fig. 7). The upper chart shows successive positions of a 500-mb. contour which was closely identified with the polar-front jet stream, while the lower chart shows consecutive locations of a contour in the general neighborhood of the subtropical jet system. At the beginning time (two days before fig. 1), the polar front was nearly coincident with the latitude of the subtropical jet near the west coast, but farther east meandered far north of it. At the end, the polar-air boundary had migrated to the latitude of the subtropical jet in the trough, while east of the trough the two currents remained separated.

The thermal structure in the cut-off Low, illustrated in

[1] Part of the analysis reported here was done while the writer was affiliated with the University of Chicago (Office of Naval Research Contract Nonr 2121 (10), NR 082-161), and with the U.S. Weather Bureau.

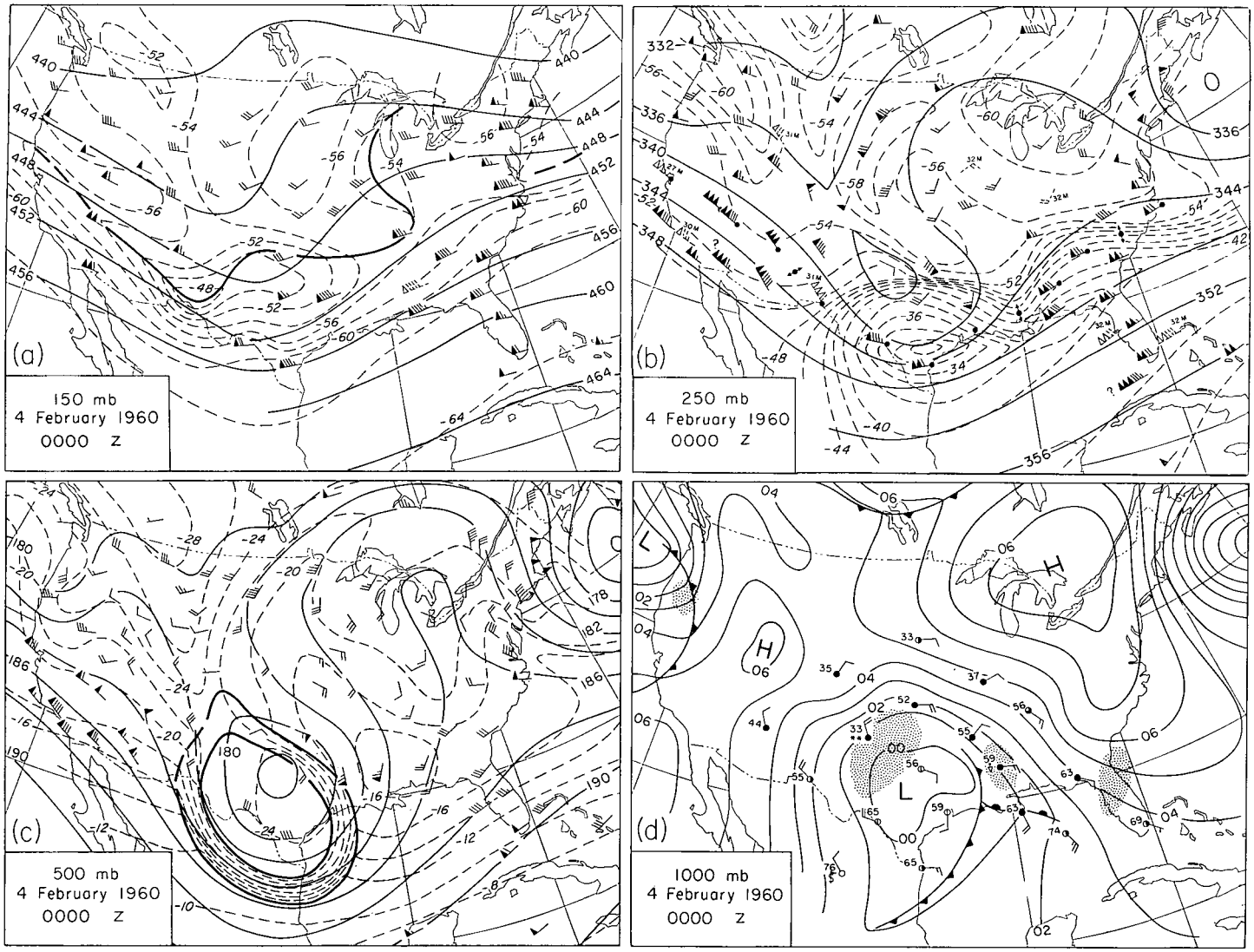

FIGURE 1.—Isobaric charts at 0000 GMT February 4, 1960: (a) 150 mb; (b) 250 mb.; (c) 500 mb.; (d) 1000 mb. In (c), frontal boundaries outlining cold-air dome are shown by heavy lines. Contours (solid lines) are at 400-ft. intervals in (a) and (b), at 200-ft. intervals in (c), and at 100-ft. intervals in (d). Isotherms (dashed lines) are at 2°C. intervals on upper-level charts.

figure 3, was indeed remarkable. A layer of great stability was present, 100 to 175 mb. in depth, with the astonishingly high temperatures of −17° C. and −16° C. at 330 and 340 mb., over Corpus Christi and Brownsville. Note that the potential temperature differences (in the vertical) between warm and cold air masses were 40° to 60° K.

The structure here is similar to that which has been shown by Mohri [4, 5] in his analyses over the vicinity of Japan. He ascribed the formation of stable layers of this kind, which achieve depths and strengths far greater than ever observed in the polar front alone, to a combination of the polar front with the "subtropical front" which is found in the upper troposphere near the subtropical jet stream.

This interpretation is borne out by figure 4, a vertical section approximately along the direction of the current at 250 mb. The soundings of figure 3 characterize the central portion of this section,[2] where the upper part of the polar-front dome osculated the subtropical front which dipped to the lowest elevation in the vicinity of the upper trough.[3]

Obviously the high temperatures near the upper part of the frontal layer could have been produced only by extreme subsidence, although the reason for the intensity of the subsidence is not evident. Vertical motions were computed from isentropic charts (not shown) at the 310° K. and 330° K. surfaces. These (see fig. 4) lay within the polar-front layer and near the middle tropopause which

[2] One of the points of similarity in the two analogous cases noted in the introduction was the nearly similar range of potential temperature through the combined frontal layer.

[3] No connection could be found between the frontal layer in the higher troposphere and the surface front (fig. 1d), which was evidently very shallow.

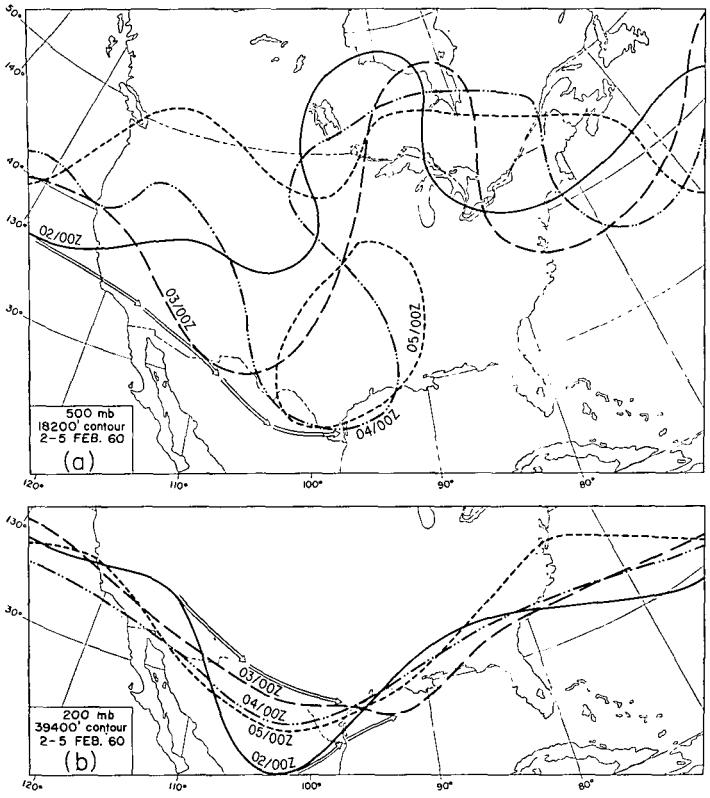

FIGURE 2.—(a) Successive locations of 18,200-ft. contour at 500 mb.; (b) locations of 39,400-ft. contour at 200 mb., at 24-hr. intervals. Double arrows in (a) show 12-hr. movement of southernmost point of contour. In (b), arrows show 12-hr. movements of ridge and trough between 0000 GMT February 2 and 0000 GMT February 3. These correspond to features which disappeared on later maps, to be replaced by a trough and a ridge farther west.

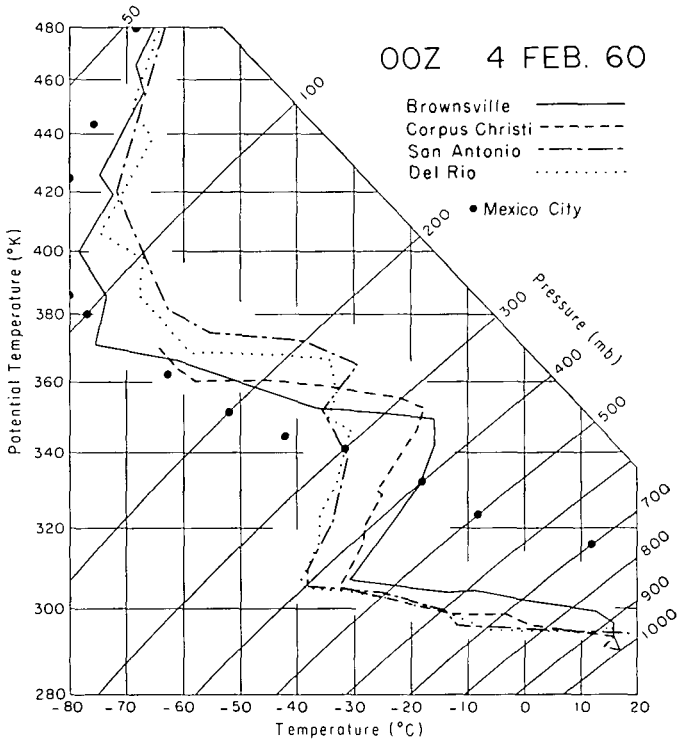

FIGURE 3.—Soundings at stations in southern Texas, at 0000 GMT February 4. Heavy dots show Mexico City temperatures at standard levels.

is identified with the lower boundary of the subtropical front. Strongest descending motions were found over El Paso at the upper of these surfaces (note, in fig. 1b, strong crossing of winds and isotherms). This amounted to $dp/dt \approx 7$ μb./sec. or $w \approx -17$ cm./sec. (near the 300-mb. level); slightly smaller values of ascending motion were found east of the trough. At the lower isentropic surface in mid-troposphere, vertical motions west of the trough did not exceed 2 to 3 μb./sec.

Thus there is evidence, in this case, that *the magnitude of vertical motions near the tropopause exceeded that in the middle troposphere.* It may further be noted (fig. 3) that lapse rates, in layers of appreciable depth above the frontal inversion, were close to the dry adiabatic. Comparison with stations upstream indicates a destabilization through vertical stretching in these levels, concomitant with the stabilization by vertical shrinking within the front.

3. SOLENOIDAL AND WIND FIELDS IN VICINITY OF TROUGH

A vertical section in the central part of the trough of figure 1, approximately normal to the strongest flow, is shown in figure 5. The frontal structure indicated south of Brownsville is partly conjectural, presumed similar to that observed 12 hr. earlier. At that time, when the polar-front zone was somewhat farther north, the observations over Texas showed a similar bifurcation of the subtropical and polar fronts in the southern part, the two frontal systems being joined farther north as in figure 5. Still farther north, between Del Rio and Amarillo, the lower boundary of the polar front was in evidence, but the upper boundary could not be distinguished from the stable air above. At Denver and Amarillo, the lower boundary of the stable layer ($\theta = 324°$ K.) corresponded to the middle tropopause which normally is continuous with the base of the subtropical front [4].

Over the whole region between Brownsville and Denver, the upper surface of the stable layer was 10° to 15° C. warmer than the undisturbed tropical air, represented by the Mexico City sounding. Over this wide range of latitude, *an abrupt reversal of the horizontal temperature gradient took place just at the upper surface of the stable layer. This was thus identified with the surface of maximum westerly geostrophic wind, which rose to high levels in the north and descended to very low elevations in the south.*[4]

[4] In this case, the wind structure was inferred from the geopotential field. In both of the analogous cases mentioned in the Introduction, direct observations showed the sheet of maximum wind was at high levels north of the jet core, and as low as the 400-mb. level south of the jet axis.

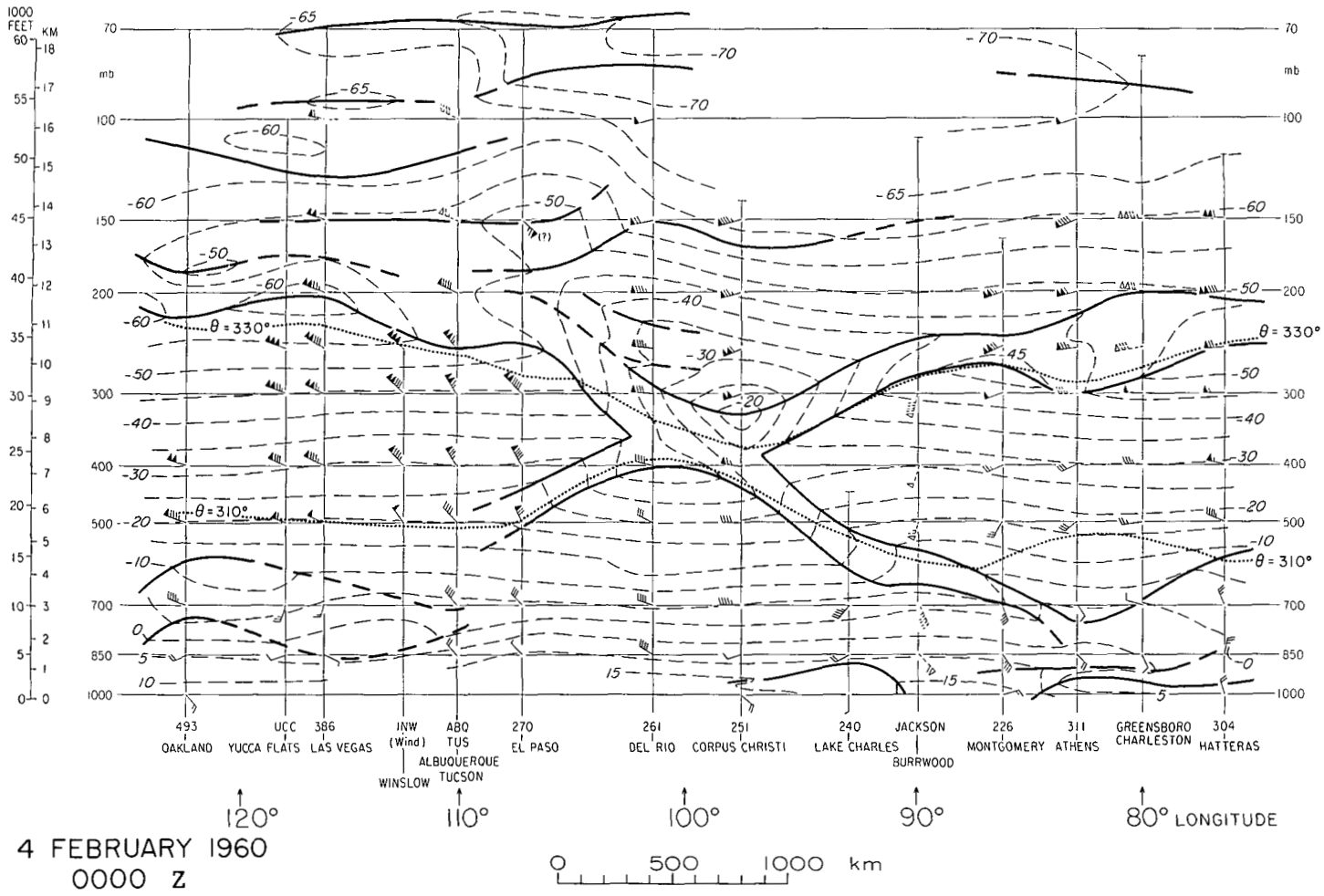

FIGURE 4.—Cross section approximately along direction of jet stream, at 0000 GMT February 4 (location of stations shown by heavy dots in fig. 1b). Heavy lines show boundaries of stable layers; dashed lines, isotherms (°C.). Wind symbols are plotted with respect to north at top of page; dotted lines correspond to 310°K. and 330°K. isentropes.

Figure 5 affords an instructive example of the relation between the vertical shear and the solenoid field. As seen from figure 1, there was not only a fairly strong curvature of the flow, but also an appreciable variation of curvature with height. Forsythe [2] has given a general equation for the variation of wind with height. Its scalar form is

$$\frac{\partial V}{\partial z}=\left(\frac{1}{f+2KV}\right)\left[f\frac{\partial V_g}{\partial z}-V^2\frac{\partial K}{\partial z}\right] \qquad (1)$$

Here V_g is the geostrophic wind speed, V the component of the real wind along V_g, K the trajectory curvature, and f the Coriolis parameter. Applications of equation (1) to the structures of subtropical and middle-latitude wave systems have been discussed in detail elsewhere [7, 8].

Where $\partial V_g/\partial z$ is very large, as within frontal layers, the last term within the brackets of equation (1) can be neglected by comparison with the first. Within the frontal layer of figure 5, the wind observation at Corpus Christi shows a mean vertical shear of 13 m./sec. per km. Averaged between Brownsville and Del Rio, the thermal shear through this layer was 28 m./sec. per km., a little over twice as great. With a mean wind speed of 38 m./sec. for the layer, and a trajectory radius of 900 km. determined from the 300- and 500-mb. charts, the ratio $f/(f+2KV)$ in equation (1) is found to be 0.45, in close agreement with the ratios of the real and thermal shears.

Above the front over Texas, the isotherms suggest a strong decay of geostrophic wind with height, whereas the actual decay was quite feeble. Over Corpus Christi, the mean geostrophic thermal shear in the layer 300–150 mb. was −9.3 m./sec. per km. compared with an average shear of the measured wind of only −1.8 m./sec. per km. Inspection of figures 1a and 1b suggests that the variation of curvature with height cannot be neglected here, where the cyclonic curvature decreases with height. This variation reflects the circumstance that the trough was much warmer at these levels, than were the ridges up- and down-stream.

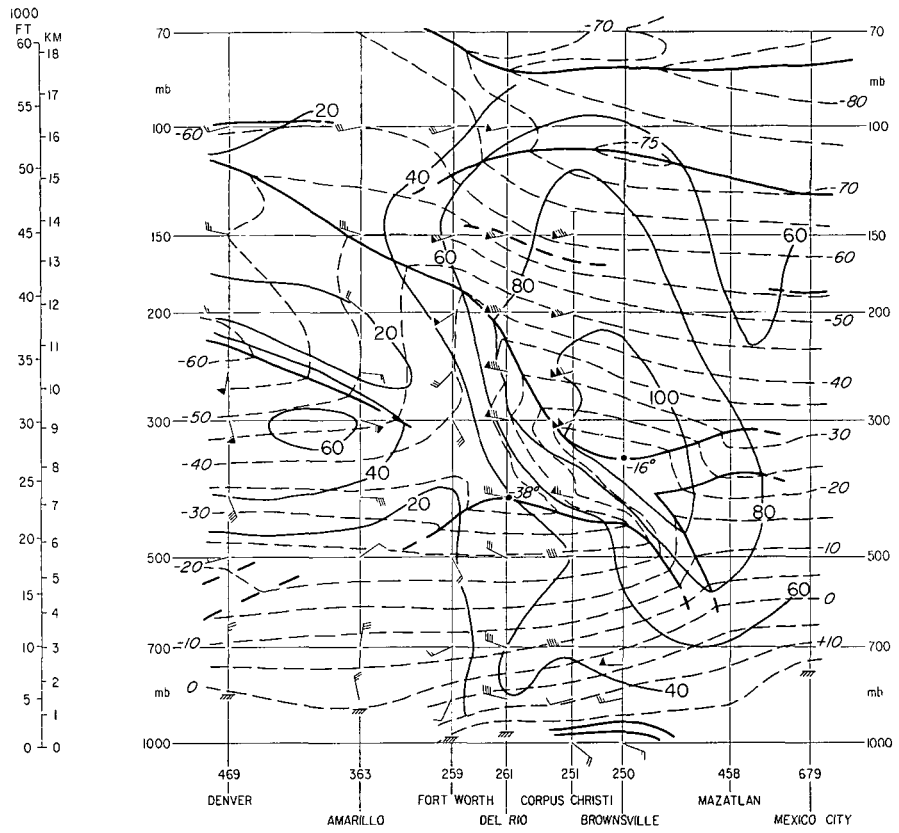

FIGURE 5.—Section approximately normal to strongest flow in trough line at 0000 GMT February 4. Dashed lines are isotherms (°C.); solid thin lines, isotachs (kt.) of total wind speed.

If α is the direction of the geostrophic wind, measured counterclockwise from east, and distance along an isobaric contour is denoted by l, the horizontal curvature of the contour is $K_l=\partial\alpha/\partial l$, and

$$\frac{\partial K_l}{\partial z}=\frac{\partial}{\partial z}\left(\frac{\partial\alpha}{\partial l}\right)=\frac{\partial}{\partial l}\left(\frac{\partial\alpha}{\partial z}\right) \tag{2}$$

In figure 6, $\mathbf{V}_T$ denotes the thermal-wind vector through a layer of thickness δz, and V_{TN} is the component of thermal wind normal to the contour direction. From the diagram, the change of contour direction through the layer is $\delta\alpha=V_{TN}/V_g$. Since from the thermal wind equation $V_{TN}=\delta z\cdot g(fT)^{-1}(\partial T/\partial l)_p$ we can write

$$\frac{\partial\alpha}{\partial z}=\frac{g}{fTV_g}\frac{\partial T}{\partial l}$$

On substitution into equation (2),

$$\frac{\partial K_l}{\partial z}\approx\frac{g}{fTV_g}\frac{\partial^2 T}{\partial l^2} \tag{3}$$

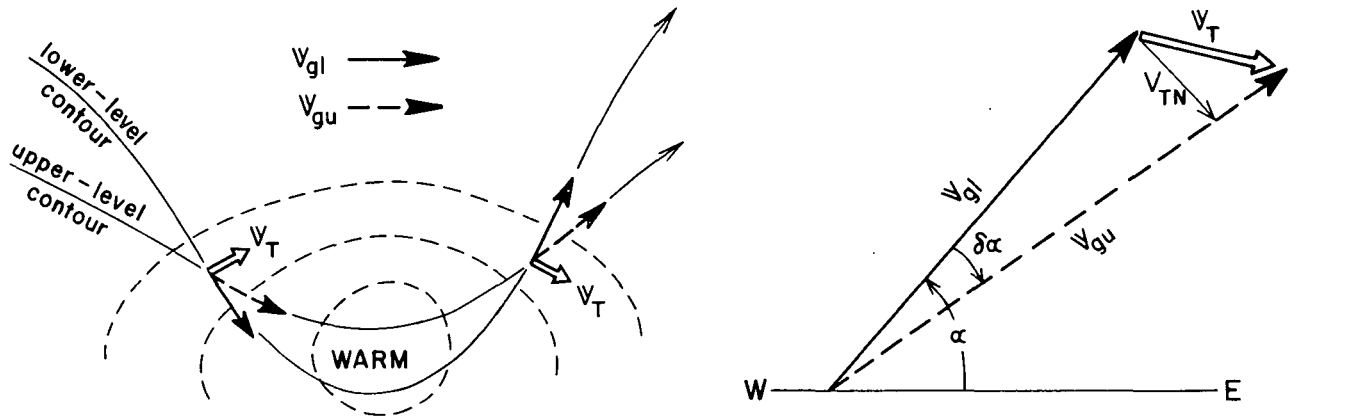

FIGURE 6.—Variation of contour curvature with height in relation to thermal wind. In detail at right, V_{gl} is the geostrophic wind at lower level, V_{gu} at upper level; V_T is thermal wind. See text.

An evaluation utilizing the mean of conditions at the 150- and 250-mb. levels (fig. 1), with the temperature gradients measured over increments of 1000 km. upstream and downstream from the trough line near the jet stream, gives $\partial^2 T/\partial l^2 \approx 15\times10^{-12}$ deg. m.$^{-2}$. Substituting $V_g=90$ m./sec. in equation (3) gives $\partial K_t/\partial z \approx 1.1\times10^{-10}$ m.$^{-2}$. Analyses based on observed wind directions indicated that the geodesic radius of curvature [9] was about 700 km. at 300 and 250 mb., and 1200 km. at 150 mb. The corresponding value of $\partial K_s/\partial z$ agrees fairly well with the variation of contour curvature with height, computed above. Although the streamline curvature was greater than that of the contours, this was true at all levels in the layer.

The purpose of the above exercise is to emphasize that *wherever the thermal gradient is large and the isotherms do not parallel the contours, the possibility must be considered that the vertical wind variation is influenced by the variation of flow curvature with height.* Although extreme, the thermal distribution in figure 1b is characteristic of the lower stratosphere near troughs.

A computation above the upper frontal surface, based on equation (1), gives a contribution from the first term of −4.1 m./sec. per km., and from the second term of +1.7 m./sec. per km. The resulting net value for $\partial V/\partial z$ is −2.4 m./sec. per km., which agrees well with the actual shear. Note that in this case, since the curvature was cyclonic, the factor in the first parentheses of equation (1) diminished the shear (by a factor of 2.3). In addition, the two terms in the second parentheses were opposed in sign. The combination of these circumstances accounts adequately for the difference, by a factor of 5, between the real and the thermal (geostrophic) shear.

4. ASYMMETRIES IN STRUCTURE

There were very marked asymmetries in the structure of both the wind and thermal fields with respect to the trough over central North America. These changed with time, in a manner somewhat similar to what is observed in middle-latitude troughs as mentioned in the Introduction.

Discontinuous retrogression of wind-speed maxima.—Figure 7 shows the flow pattern at the 200-mb. level, at 12-hr. intervals from 0000 GMT February 2 through 0000 GMT February 5, 1960. A cursory inspection reveals that throughout this period, there was a trough in lower latitudes near 100° W., and regions of maximum wind in the southwestern and southeastern United States.[5]

Between the times of figures 7b and 7e, the initial lower-latitude trough (which had been moving eastward at about 25 kt.) was replaced by another trough, which deepened farther west while the original trough moved eastward and filled. This change, although much more subtle in terms of magnitude, is similar to the process that takes place when a middle-latitude minor trough moves into the long-wave major trough position [1, 10]. The retrogression in the subtropical trough was effected in harmony with the deepening, in this location, of the polar trough which had entered the west coast around 0000 GMT February 2.

The overall changes in configuration of the contour representing the subtropical wind system (fig. 2) were very modest, during this 3-day period, in comparison with the large shifts of position of the polar-front-current systems. Nevertheless, changes of the wind field were quite pronounced, as may be seen by inspection of the jet streaks near the east and west coasts. Two of the more striking changes are *the discontinuous retrogression of the western jet streak between figures 7a and 7b, and the subsequent retrogression of the eastern one between figures 7d and 7e.*

Because of the rapidity of the changes and the availability of adequate wind observations only at 12-hr. intervals, it is not possible to examine the details of these retrogressions. However, it may be pointed out that they followed a regular sequence with the retrogressive redevelopment of the subtropical trough. From inspection of figure 7, the discontinuous westward shift of this trough appears to have been centered roughly at 0000 GMT February 3; the jet-streak retrogressions on the western and eastern sides took place about 18 hr. before and after this time. This would correspond to an eastward speed of the retrogressive "impulse" of about 60 kt., which is roughly equivalent to the group velocity of Rossby waves in winter.

Note that in contrast to the most common pattern in developing middle-latitude troughs ([10], pp. 28–29), the jet streak on the western side did not migrate through the subtropical trough to the eastern side. The behavior in the present case is characteristic of the subtropical jet stream, in which (see, e.g., [3]) it is very difficult to dislodge the wind maxima from the crests.

The subtropical front.—Comparison of figures 8a and 8b, two sections in the ridges west and east of the subtropical trough, indicates that the frontal structure was asymmetrical. At this time, *prior to the retrogression of the subtropical trough, the subtropical front was very prominent on the western side but virtually absent on the eastern side.* Thirty-six hours later (figs. 8c and 8d), *following the retrogression, the situation was reversed, with a very strongly developed subtropical front on the eastern side of the trough.* This front was unusually pronounced, with an overall temperature contrast up to about 15° C., which is comparable to the contrast observed across a strong polar front in the upper troposphere. Its slope, as is perhaps to be expected because of the low latitude and anticyclonic curvature, was about ½₀₀ to ⅓₀₀, or appreciably weaker than the typical slope of the upper-tropospheric polar front.

It is not possible to examine the details all along the

[5] These local concentrations of higher speed, such as the one shown by the isotachs centered about Charleston in figure 7c, will here be called "jet streaks", in distinction to "jet stream" which refers to the current of maximum wind as a whole.

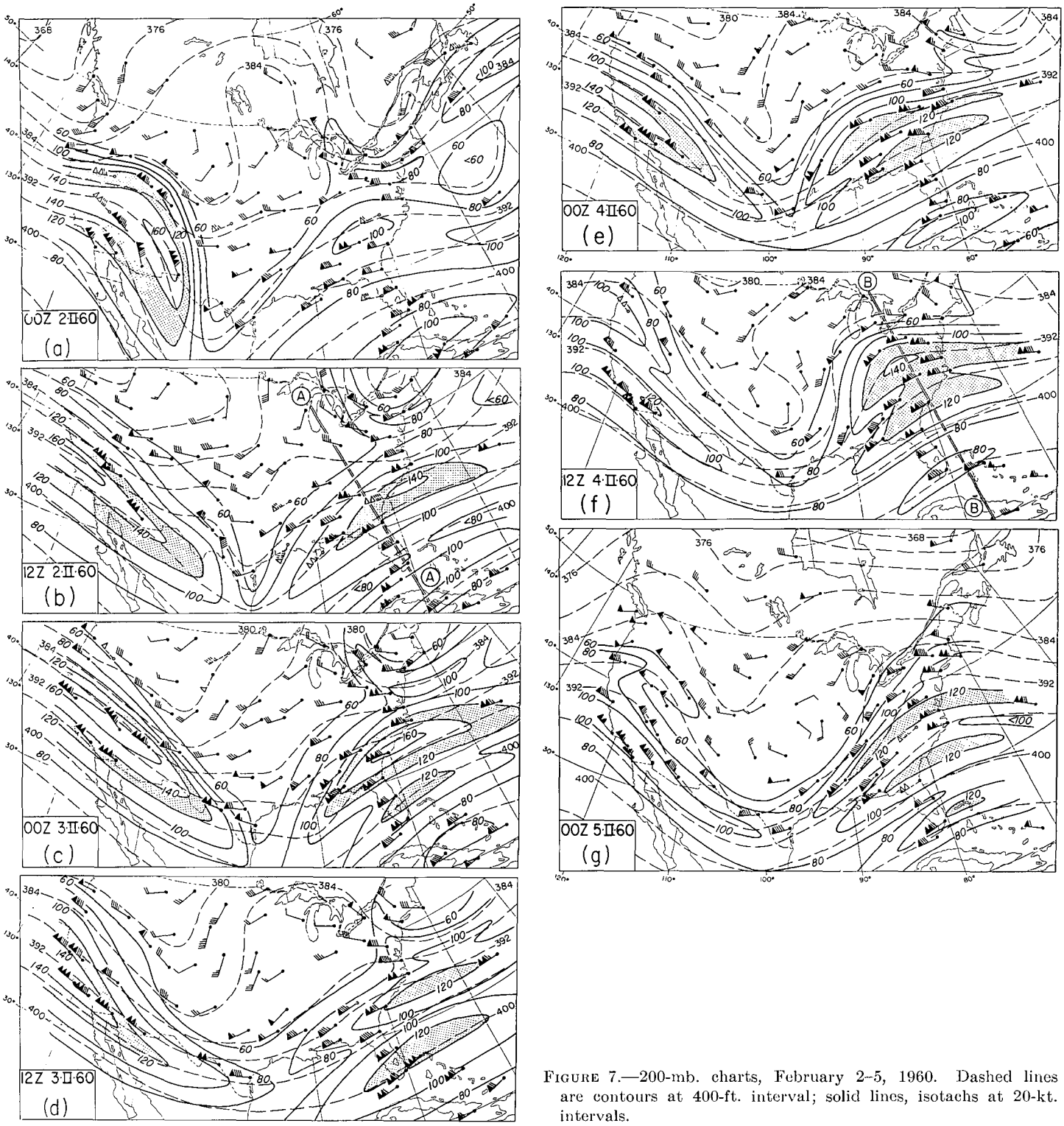

FIGURE 7.—200-mb. charts, February 2–5, 1960. Dashed lines are contours at 400-ft. interval; solid lines, isotachs at 20-kt. intervals.

current, because of the limited network in lower latitudes. However, it appears (from this and other cases) that the frontal asymmetries characteristic of middle-latitude troughs are also characteristic of the subtropical-current system, when polar-air troughs interact with it.

Figures 8b and 8c are similar in that the subtropical tropopause "A," in the vicinity of 200 mb. near the subtropical jet, was quite well marked. In figures 8a and 8d *where the subtropical front was very strongly developed, the subtropical tropopause was weak or absent.* The presence or absence of this tropopause, below the real tropical tropopause, reflects a difference in stability through a deep layer of the upper tropical troposphere. This can be appreciated from a comparison of the vertical spacing

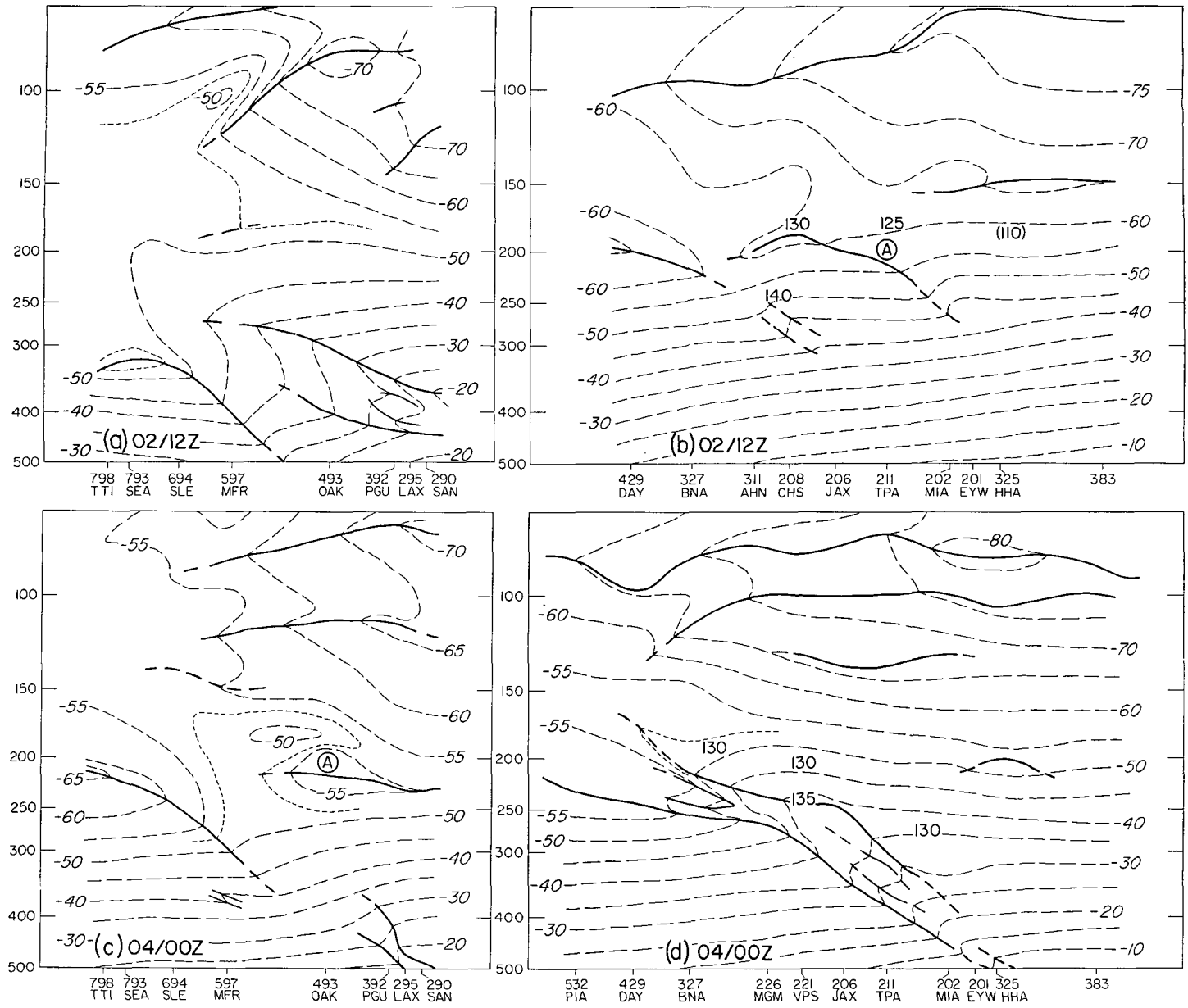

FIGURE 8.—Cross sections near west coast (left) and approximately along ridge over eastern United States and Caribbean (right), at 1200 GMT February 2 (top) and 0000 GMT February 4 (bottom). Heavy lines mark boundaries of stable layers or tropopauses; dashed lines are isotherms (°C.). In right-hand sections, upright numbers show speeds (kt.) and locations of jet-stream cores.

of the isotherms in the upper central portions of figures 8b and 8d. The same sort of contrast, between the western ridge where the subtropical front was absent and the eastern ridge where it was strong, is illustrated by the composite soundings at 1200 GMT February 4 in figure 9.

As illustrated by figure 10, the varying degree of development of the subtropical front was connected with differences of the thermal and kinematic structures over a broad region. At 1200 GMT February 2 (fig. 10a) when the subtropical front was absent, the surface of maximum wind was nearly horizontal. Two days later when the front was strong, the air above its upper surface was appreciably warmer than the undisturbed tropical air to the south. *The surface of reversal of baroclinity was thus near the upper frontal surface, and the surface of maximum wind had a marked downward tilt toward the south.* This feature was also present in the other cases mentioned in the Introduction.[6]

A change of this general sort appears to be a necessary concomitant of strong subtropical front development.

[6] It is appropriate to note that a tilt of the surface of maximum wind downward toward the south is sometimes observed even when this is not indicated by the baroclinic field. This is an influence of inertial motions, and has been discussed in detail by Newton and Persson [7]. In figure 10, and in analogous sections in the ridge at other times, the increase of wind speed with height below, or the decay above, the subtropical jet stream was up to 2 to 3 times stronger than the geostrophic thermal wind. This is due to influences of curvature in the ridges, in accord with equation (1).

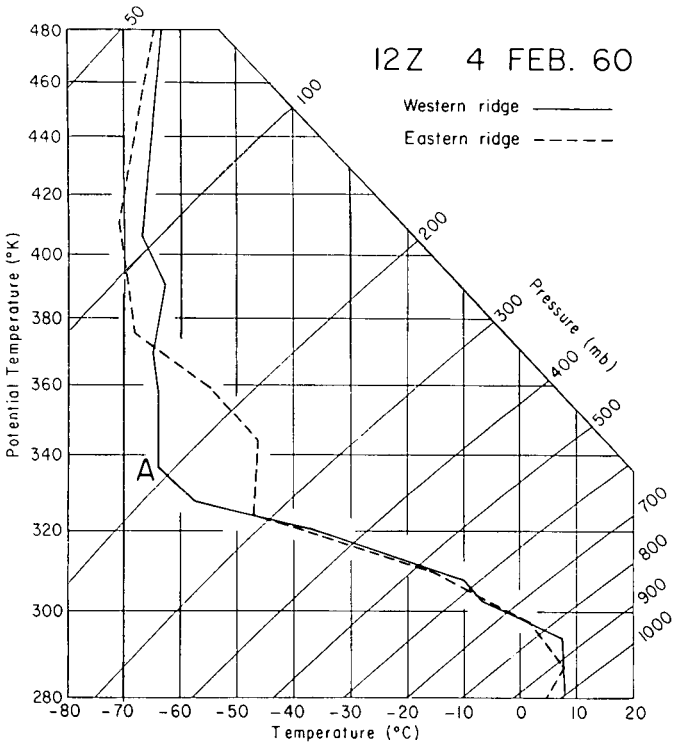

FIGURE 9.—Composite soundings near jet stream at 1200 GMT February 4, in the western (solid) and eastern (dashed) ridges. The solid curve is a composite of stations 290, 386, 392, 493; the dashed curve represents stations 206, 208, 304, 308, 317, 403, and 520. "A" is the subtropical tropopause, identified in figure 8c.

The overall temperature contrasts between undisturbed tropical and middle-latitude air masses, and the overall temperature lapse between the middle troposphere and the level of the tropical tropopause, are relatively fixed. This being the case, *a concentration of a large part of the baroclinity and stability within a frontal layer must take place at the expense of the baroclinity and stability in the air masses bounding the front.* The creating of a well-developed front thus has significant accompaniments in the thermal (and kinematic) structures over a considerable region embracing the front, not just in the immediate vicinity of the front itself

5. CONCLUSION

One objective of this analysis study has been to emphasize the large degree of variation in the structure of the thermal and wind fields in different parts of the subtropical wave system, and at different times. Saucier [11] has cautioned against a too-ready acceptance of "models" or of categorical statements about the features of the subtropical jet stream, since the structure varies greatly from one case to another. Thus, for example, although the level of maximum wind in the subtropical stream is most often found near 200 mb. (40,000 ft.), in some situations it may be as low as 300–400 mb. or 10,000–15,000 ft. lower (as illustrated by figs. 5 and 10b). Also the strength of the subtropical front may be very

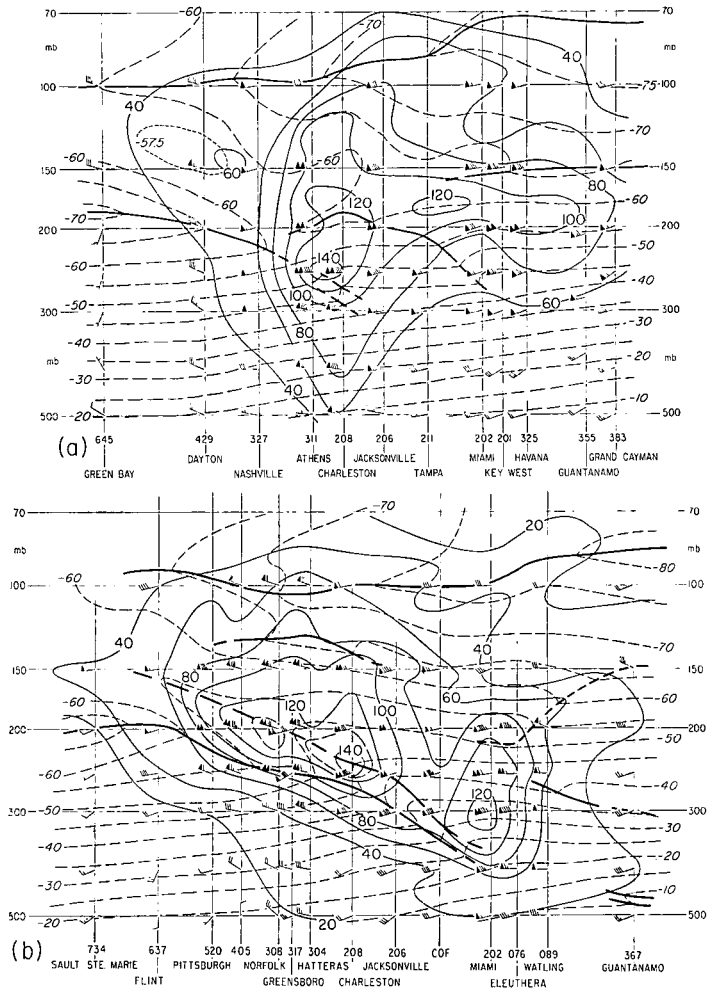

FIGURE 10.—Cross sections in ridge over eastern North America, (a) 1200 GMT February 2; (b) 1200 GMT February 4. Section (a) is along line AA in figure 7b; section (b) is along line BB in figure 7f.

different in diverse situations, with accompanying variations in the temperature and stabilities in the upper tropical troposphere.

Another purpose has been to point to certain features worthy of further investigation. Thus, for example, forecasters concerned with upper winds are certain to be familiar with the fact that discontinuous retrogression of the regions of maximum wind in the subtropical jet stream is a fairly common event. Yet very little appears in the literature, either in the way of description or explanation, concerning this phenomenon. It often appears, as in the case described above, that such jet-streak retrogressions occur (as do retrogressions of the middle-latitude waves) successively downstream from one another. Because adequate aerological networks cover such small longitudinal sectors in the subtropics, it is difficult to arrive at any systematic description of this process. Nevertheless the suggestion is clear, that events in one portion of the subtropical latitudes are very likely affected by other events in distant locations, both within the subtropics and at higher latitudes.

REFERENCES

1. G. P. Cressman, "On the Forecasting of Long Waves in the Upper Westerlies," *Journal of Meteorology*, vol. 5, No. 2, Apr. 1948, pp. 44–57.
2. G. E. Forsythe, "A Generalization of the Thermal Wind Equation for Arbitrary Horizontal Flow," *Bulletin of the American Meteorological Society*, vol. 26, No. 10, Dec. 1945, pp. 371–375.
3. T. N. Krishnamurti, "The Subtropical Jet Stream of Winter," *Journal of Meteorology*, vol. 18, No. 2, Apr. 1961, pp. 172–191.
4. K. Mohri, "On the Fields of Wind and Temperature over Japan and Adjacent Waters During Winter of 1950–51," *Tellus*, vol. 5, No. 3, Aug. 1953, pp. 340–355.
5. K. Mohri, "Jet Stream and Upper Fronts in the General Circulation and their Characteristics over the Far East," *Geophysical Magazine* (Tokyo), vol. 29, No. 1, Nov. 1958, pp. 45–126 (part I), and vol. 29, No. 3, Aug. 1959, pp. 333–412 (part II).
6. C. W. Newton, "Variations of Frontal Structure of Upper Level Troughs," *Geophysica*, vol. 6 (Palmén 60th anniversary volume), Nos. 3–4, Aug. 1958, pp. 357–375.
7. C. W. Newton and A. V. Persson, "Structural Characteristics of the Subtropical Jet Stream and Certain Lower Stratospheric Wind Systems," *Tellus*, vol. 14, No. 2, May 1962, pp. 221–241.
8. C. W. Newton and E. Palmén, "Kinematic and Thermal Properties of a Large-Amplitude Wave in the Westerlies," *Tellus*, vol. 15, No. 2, May 1963, pp. 99–119.
9. G. W. Platzman, "Some Remarks on the Measurement of Curvature and Vorticity," *Journal of Meteorology*, vol. 4, No. 2, Apr. 1947, pp. 58–62.
10. H. Riehl and Collaborators, "Forecasting in Middle Latitudes," *Meteorological Monographs*, American Meteorological Society, Boston, vol. 1, No. 5, June 1952, 80 pp.
11. W. J. Saucier and Collaborators, "Wind Field Near the Tropopause," *Final Report*, Contract AF 19(604)–1565, Agricultural and Mechanical College of Texas, December 1958, 140 pp.

[*Received July 20, 1964*]

CORRESPONDENCE

Comments on "Some Problems Involved in the Numerical Solutions of Tidal Hydraulics Equations"

GÜNTER FISCHER

Meteorologisches Institut, Hamburg 13, West Germany

In an article by Harris and Jelesnianski [1] several references were made to a finite difference approximation to the hydrodynamic equations which I have employed for tidal and wind-stress computations in the North Sea [2]. In the same notation as in [1], the scheme reads as follows:

$$U_{i,j}^{m+1}=U_{i,i}^{m}-\frac{g\Delta t}{2\Delta s}D_{i,j}[h_{i+1,j}^{m}-h_{i-1,j}^{m}]+\Delta t\,[fV_{i,j}^{m}]$$

$$V_{i,j}^{m+1}=V_{i,j}^{m}-\frac{g\Delta t}{2\Delta s}D_{i,j}[h_{i,j+1}-h_{i,j-1}]-\Delta t\,[fU_{i,j}^{m}]$$

$$h_{i,j}^{m+1}=h_{i,j}^{m}-\frac{\Delta t}{2\Delta s}[U_{i+1,j}^{m+1}-U_{i-1,j}^{m+1}+V_{i,j+1}^{m+1}-V_{i,j-1}^{m+1}] \quad (1)$$

This scheme is stable if $f=0$ provided $\Delta t<\sqrt{2/(gD)}\Delta s$ but unfortunately gives rise to growing solutions if rotation is involved. (The maximum eigenvalue is $|\lambda_{\max}|=\sqrt{1+f^2\Delta t^2}$). Instability was indeed observed by the authors in a test computation (fig. 2 in [1]).

Since scheme (1) has the great advantage, in contrast to the commonly used central difference scheme ((16), (17), (18) in [1]), that only field values at time $(m-1)$ Δt are required it seems worthwhile to try to remove the shortcomings of scheme (1). This is easily done if in (1) the Coriolis terms are centered in time so that $f\Delta tU_{i,j}^{m}$ and $f\Delta tV_{i,j}^{m}$ are replaced by $\frac{1}{2}(f\Delta tU_{i,j}^{m+1}+f\Delta tU_{i,j}^{n})$ and $\frac{1}{2}(f\Delta tV_{i,j}^{m+1}+f\Delta tV_{i,j}^{m})$ respectively. In this way the scheme becomes implicit. If a grid is used, however, where both U and V are defined at the same grid points, only a system of two algebraic equations has to be solved for the unknowns $U_{i,j}^{m+1}$ and $V_{i,j}^{m+1}$. Thus the new scheme can be written

$$U_{i,j}^{m+1}-\frac{f\Delta t}{2}V_{i,j}^{m+1}=U_{i,j}^{m}-\frac{g\Delta t}{2\Delta s}D_{i,j}$$
$$[h_{i+1,j}-h_{i-1,j}]+\frac{f\Delta t}{2}V_{i,j}^{m}\equiv X_{i,j}^{m}$$

$$V_{i,j}^{m+1}+\frac{f\Delta t}{2}U_{i,j}^{m+1}=V_{i,j}^{m}-\frac{g\Delta t}{2\Delta s}D_{i,j}$$
$$[h_{i,j+1}-h_{i,j-1}]-\frac{f\Delta t}{2}U_{i,j}^{m}\equiv Y_{i,j}^{m}$$

$$U_{i,j}^{m+1}=\frac{1}{1+\frac{f^2\Delta t^2}{4}}\left[X_{i,j}^{m}+\frac{f\Delta t}{2}Y_{i,j}^{m}\right] \quad (2)$$

$$V_{i,j}^{m+1}=\frac{1}{1+\frac{f^2\Delta t^2}{4}}\left[Y_{i,j}^{m}-\frac{f\Delta t}{2}X_{i,j}^{m}\right]$$

$$h_{i,j}^{m+1}=h_{i,j}^{m}-\frac{\Delta t}{2\Delta s}[U_{i+1,j}^{m+1}-U_{i-1,j}^{m+1}+V_{i,j+1}^{m+1}-V_{i,j-1}^{m+1}]$$